

AMMRC TR 85-28

Boyd
MONTGOMERY

AD

ENVIRONMENTAL ASSISTED CRACKING IN HIGH HARDNESS ARMOR STEEL

WILLIAM A. HERMAN and GLENN M. CAMPBELL
PROCESS RESEARCH DIVISION

September 1985

Approved for public release; distribution unlimited.

ARMY MATERIALS AND MECHANICS RESEARCH CENTER
Watertown, Massachusetts 02172-0001

The findings in this report are not to be construed as an official Department of the Army position, unless so designated by other authorized documents.

Mention of any trade names or manufacturers in this report shall not be construed as advertising nor as an official indorsement or approval of such products or companies by the United States Government.

DISPOSITION INSTRUCTIONS

Destroy this report when it is no longer needed.
Do not return it to the originator.

SECURITY CLASSIFICATION OF THIS PAGE (When Data Entered)

REPORT DOCUMENTATION PAGE		READ INSTRUCTIONS BEFORE COMPLETING FORM	
1. REPORT NUMBER AMMRC TR 85-28		2. GOVT ACCESSION NO. 	
		3. RECIPIENT'S CATALOG NUMBER 	
4. TITLE (and Subtitle) ENVIRONMENTAL ASSISTED CRACKING IN HIGH HARDNESS ARMOR STEEL		5. TYPE OF REPORT & PERIOD COVERED Final Report	
		6. PERFORMING ORG. REPORT NUMBER 	
7. AUTHOR(s) William A. Herman and Glenn M. Campbell		8. CONTRACT OR GRANT NUMBER(s) 	
9. PERFORMING ORGANIZATION NAME AND ADDRESS Army Materials and Mechanics Research Center ATTN: AMXMR-MR Watertown, Massachusetts 02172-0001		10. PROGRAM ELEMENT, PROJECT, TASK AREA & WORK UNIT NUMBERS D/A Project: 1X423735D330 AMCMS Code: 24034	
11. CONTROLLING OFFICE NAME AND ADDRESS U.S. Army Materiel Command Alexandria, Virginia 22333		12. REPORT DATE September 1985	
		13. NUMBER OF PAGES 19	
14. MONITORING AGENCY NAME & ADDRESS(if different from Controlling Office) 		15. SECURITY CLASS. (of this report) Unclassified	
		15a. DECLASSIFICATION/DOWNGRADING SCHEDULE 	
16. DISTRIBUTION STATEMENT (of this Report) Approved for public release; distribution unlimited.			
17. DISTRIBUTION STATEMENT (of the abstract entered in Block 20, if different from Report)			
18. SUPPLEMENTARY NOTES			
19. KEY WORDS (Continue on reverse side if necessary and identify by block number) Environmental assisted Crack propagation Heat treatment cracking Stress relaxation Steel High hardness steel Stress relieving Residual stress			
20. ABSTRACT (Continue on reverse side if necessary and identify by block number)			
SEE REVERSE SIDE			

Block No. 20

ABSTRACT

At the request of several program managers, AMMRC investigated cracking of high hardness armor steel (MIL-A-46100). Cracks were first reported on detail parts that were stored after being cut from large plates. In addition, the cracking was reported during subsequent fabrication steps, as well as in fielded vehicles.

AMMRC found an environmental assisted cracking (EAC) mechanism to be responsible for the cracking phenomenon. AMMRC further identified two significant factors which could be controlled and thereby reduce the likelihood of EAC occurring: the residual stress level in the parts, and microcrack formation at cut edges.

The residual stress level in the detail parts was related to the heat treatment of the high hardness steel. The AMMRC investigation identified a minimum tempering temperature and time (350°F/30 min) to minimize the residual stress level in the heat treated plates. These tempering parameters were incorporated into the latest revision of MIL-A-46100 in April 1983. AMMRC further recommended the best cutting procedure in order to minimize the number of microcracks on plate edges, which acted as EAC initiation sites.

CONTENTS

	Page
INTRODUCTION.	1
EXPERIMENTAL PROCEDURES	
Description of Plates.	4
Nondestructive Examination	4
Chemical Analysis.	5
Metallography.	5
Stress Relaxation.	5
Mechanical Testing	6
Environmental Assisted Cracking Tests.	6
RESULTS AND DISCUSSION.	7
Crack Initiation	7
Materials Characterization/Environmental Influence .	7
Residual Stress.	13
Tempering.	13
SUMMARY	15

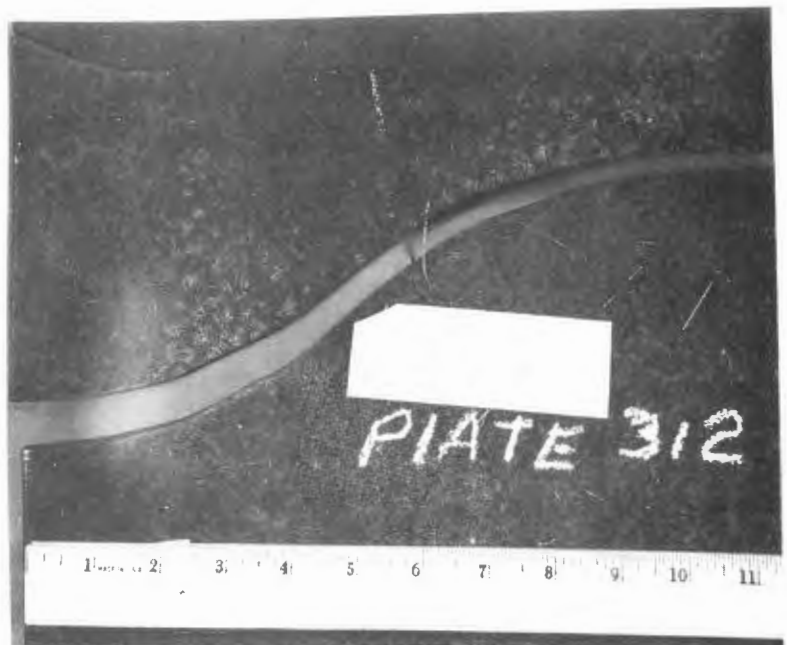
INTRODUCTION

When high hardness armor is used in combat vehicles, the material processing and fabrication sequence must be carefully planned and executed in order to avoid conditions that promote premature failure. One mechanism that can severely degrade the service life of steel components is environmental assisted cracking (EAC).¹

EAC is the stable, subcritical growth of a crack in a material under stress which is exposed to a hostile environment. The susceptibility of high strength steel to EAC is well documented¹⁻³ and when extensive cracking was observed in 5/16-inch and 3/8-inch plates of high hardness steel armor (MIL-A-46100)⁴ during vehicle construction, EAC was immediately suspected as a probable failure mode (see Figure 1). An in-depth metallurgical analysis at AMMRC revealed that EAC was the operative cracking mechanism, with crack propagation occurring through the interaction of edge cracks with the ambient environment (moist air) and plate residual stresses (due to thermal cutting and insufficient tempering).



Part 312



Part 312, Close-up of Cracked Area

Figure 1. Catastrophic Cracks in Detail Parts.

1. FLETCHER, E., BERRY, W., and ELSEA, A. *Stress Corrosion Cracking and Hydrogen Cracking of High Strength Steel*. DMIC Report 232, July 29, 1966.
2. DAWSON, D. B., LEVY, M., and SEITZ, D. W. *Stress Corrosion Cracking of High Hardness Steel Armor* in Proceedings of the Tri-Service Corrosion of Military Equipment Conference, v. 2, Sessions 4-7, October 1974, Dayton, Ohio.
3. MOSTOVOY, S., and RIPLING, E. *The Feasibility of Using Fracture Mechanics for Evaluating High Hardness Armor Steel*. Final Technical Report Contract DAAE07-68-C-2305, TACOM, June 1969.
4. MIL-A-46100, *Armor Plate, Steel, Wrought, High Hardness*, June 1983, Prepared by Army Materials and Mechanics Research Center.

The following four conditions must be met in order for environmental assisted cracking to occur.

1. A crack initiation event must have occurred.
2. The component must be under stress (applied or residual).
3. The component must be exposed to an aggressive environment.
4. The material must possess an inherent susceptibility to environmental assisted crack propagation (e.g., a K_{IEAC} threshold well below the K_{IC}).

However, the EAC phenomenon can be effectively eliminated if any of these four conditions can be removed, or adequately controlled,⁵ e.g., if thermomechanical treatments can reduce the plates residual stress level, or if the structure can be redesigned so that the applied stress is lowered, no EAC will be seen even though a crack may be present in a susceptible material which is exposed to a harsh environment. (Table 1 shows the interdependence of the four controlling factors.)

In addition to understanding the interrelationship of these four necessary conditions, the dynamic nature of EAC can be understood by examining the relative values of the instantaneous stress intensity at the crack tip (K_i), the plane-strain fracture toughness (K_{IC}) and the environmental assisted cracking fracture toughness (K_{IEAC}). When the values of these three stress intensities for a given material/environment system are compared to each other, the exact nature of crack propagation during EAC can be easily understood.

The following three situations represent the boundary conditions that define the nature of EAC:

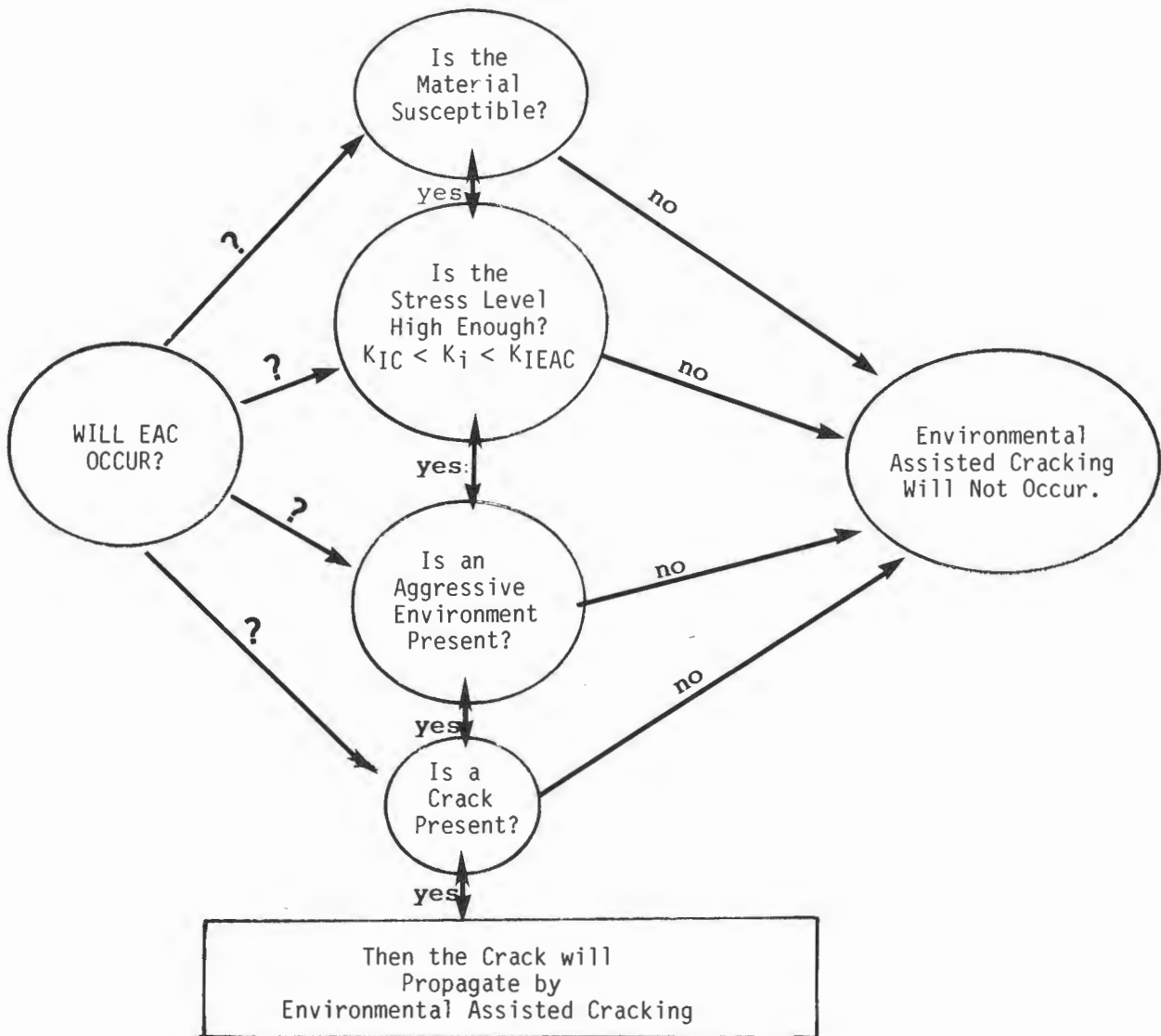
1. $K_i > K_{IC}$
2. $K_i < K_{IEAC}$
3. $K_{IEAC} < K_i < K_{IC}$

In the first case, the crack tip stress intensity is greater than the materials fracture toughness. Immediate catastrophic fracture of the material will occur upon initial loading to K_i because the materials fracture toughness (K_{IC}) has been exceeded. For the case where $K_i < K_{IEAC}$, there will be no crack extension, because the prevailing stress intensity (K_i) is not a sufficient driving force to cause the crack to propagate.

EAC will occur when the crack tip stress intensity is between the EAC threshold and the fracture toughness. Under these conditions, a crack will grow in a stable manner at a rate characteristic of the material/environment system.⁵ The final fracture characteristics will be dependent on whether the stress is applied externally, or is residual within the plate. When the stress is external, the crack tip stress intensity (K_i) increases as the crack grows, and when K_i reaches K_{IC} catastrophic fracture of the component will occur. However, when the stresses are residual due to prior fabrication processes, an entirely different situation is encountered. In this case, the residual stresses are relieved as the crack extends, and K_i may not necessarily increase to the K_{IC} because increases in crack

5. HERTZBERG, R. W. *Deformation and Fracture Mechanics of Engineering Materials*. Wiley & Sons, New York, 1976, Chapter 11, p. 377-411.

Table 1. INTERRELATIONSHIP OF NECESSARY CONDITIONS FOR ENVIRONMENTAL ASSISTED CRACKING



length are offset by decreases in the stress level. If K_i does not reach K_{IC} , crack growth will continue to occur in a slow, stable manner, with no fast fracture ever occurring. This situation accurately describes the cracking problems encountered during vehicle production. AMMRC's experimental work fully characterized this EAC phenomenon and identified changes in production techniques that reduce the likelihood of EAC when high hardness armor is used in future combat vehicles.

EXPERIMENTAL PROCEDURES

Description of Plates

Material used in the study included five 5/16-inch-thick parts from the vehicle production line. In addition, a variety of test plates (12" x 12" x 5/16") from cracked and uncracked material were examined. Most of these were given stress relief heat treatments after cutting, and were evaluated to ensure that the stress relief did not degrade performance.

Table 2 lists the sizes and quantities of the plates received, and also includes a brief description of the plates condition. The identification given in Table 2 will be used throughout the remainder of this report.

Nondestructive Examination

The cracked parts (312, 313A, 313B, 313C) were examined with fluorescent magnetic particle inspection (MPI) in order to detect the extent and morphology of microcracks along cut surfaces.

Table 2. LIST OF MATERIALS*

Plate/Part Ident. No.	Qty.	Thick.	Size	Condition
312	1	5/16"	26" x 49"	as-cracked - water-shielded plasma cutting
313A,B&C	3	↓	24" x 26"	as-cracked - cold-sheared oxyfuel cut-out notch
309	1		24" x 26"	uncracked - gas-shielded plasma cut
1-5	5		12" x 12"	from plate with cracked parts SR [†] 350°F/1 hr
6-7	2			from plate with uncracked parts SR 400°F/1 hr
8-9	2			SR 450°F/1 hr
10-11	2			SR 500°F/1 hr
12-13	2			SR 550°F/1 hr
14-17	4			no SR
18	1			SR 400°F/1 hr
19	1			SR 450°F/1 hr
20	1			SR 500°F/1 hr
21	1			SR 550°F/1 hr
22-23	2			no SR
D	1			standard heat treatment with no SR

*The steels studied can be divided into two alloy combinations. The first steel is a manganese (Mn)-Molybdenum (Mo)-Boron (B) alloy. All of the parts and most the plates are of this chemistry. Another high hardness steel chemistry uses Nickel (Ni) and Chromium (Cr) as the major alloy elements. Plate D is of this alloy. Both of the steel chemistries use a nominal 0.30 weight percent carbon (C) as is allowed by specification MIL-A-46100. Table 4 gives representative chemistry ranges of both classes of high hard, as well as the specific information that is relevant to one of the cracked parts.

†SR - stress relief

The stress-relieved test plates and part 309 were also examined with MPI in order to detect the cracking severity.

Chemical Analysis

Chemical analysis was performed on chips milled from cracked part 313C and plate D. The analysis of the carbon and sulphur was performed by combustion and later verified by infrared carbon analysis. All other elements were evaluated with emission spectrometry. Part 313C represented the Mn-Mo-B chemistry while plate D was of the Ni-Cr chemistry (see Table 3).

Metallography

Optical metallography was used to examine cut edge microstructure, bulk steel microstructure, and any crack morphology/microstructure correlation. In addition, the scanning electron microscope (SEM) was used to characterize the actual crack fracture surfaces and broken Charpy and tensile bar surfaces. All of the optical metallography samples were prepared using standard metallographic practices. The optical specimens that were examined included a series of plate edges to compare various cutting techniques (water-shielded plasma, gas-shielded plasma, and cold shearing). The edges were studied for any microstructural and microhardness variations with distance from the edge to determine the effects of each cutting process. The bulk microstructure of each steel chemistry (Mn-Mo-B and Ni-Cr) was also examined. Finally, crack morphology was analyzed at various stages of crack development; initiation less than 0.04", 2", and 7" with particular interest focused on corrosion products, if any, located within the crack tip.

Stress Relaxation

A series of fixed displacement load relaxation tests were performed to determine the effects of tempering temperature on the residual stress in high hardness steel plates. Threaded round tension specimens (gage diameter = 0.160", gage length 0.64") were machined from part 313C, and these specimens were loaded in a 20,000-pound capacity Instron tension testing machine that was equipped with a

Table 3. CHEMISTRY DATA ON HIGH-HARD STEEL

	C	Mn	P	S	Ni	Cr	Al	Mo	Si	B
313C Mn-Mo-B	0.33	1.41	0.008	0.009	0.002	0.038	-	0.19	-	0.005
D Ni-Cr	0.30	0.92	0.009	0.011	0.98	0.55	0.031	0.50	0.44	-
4340*	0.38/0.43	0.6/0.8	0.035 max	0.040 max	1.65/2.00	0.7/0.9	0.2/0.3	0.15/0.3	-	-
J13 (Ref. 2)	0.30	1.20	0.012	0.020	-	0.02	-	0.21	0.24	-
G11 (Ref. 2)	0.28	0.94	0.010	0.025	-	0.59	-	0.21	0.66	-
MIL-A-46100B	0.28/0.32	-	0.025 [†] max	0.025 [†] max	-	-	-	-	-	-

*ASM Metals Handbook, v. 1, 9th edition, 1978.

[†]Total percent phosphorous and sulphur may not exceed 0.040.

furnace capable of maintaining specimen temperatures from 100°F to 400°F. The test procedure involved establishing the furnace temperature and then loading the specimens to a predetermined initial stress. The crosshead of the testing machine was then locked at a fixed displacement and the load relaxation was measured as a function of time. Initial stress levels were kept below the yield strength of the steel to accurately simulate bulk plate residual stress levels. The test temperatures ranged from 150°F to 400°F in order to span the typical tempering temperature range for high hardness steel. The test matrix of initial stress and test temperatures is given in Table 4.

Table 4. TEST MATRIX OF STRESS RELAXATION STUDY

Initial Stress (ksi)	Test Temperature (°F)					
	150	200	250	300	350	400
100						
200						

Mechanical Testing

Fracture toughness tests were performed on both part 313C (Mn-Mo-B grade) and plate D (Ni-Cr grade) of high-hard steel according to ASTM E399-81. The tests used precracked Charpy bars loaded in three-point bending, and the results obtained were compared to the criterion of ASTM E399-81 section 7.1.1 to verify that a valid plane-strain fracture toughness had been obtained.

Longitudinal and transverse tension tests (ASTM E8-81) utilizing flat dogbone specimens, and subsize Charpy impact tests (ASTM 23-81) were performed on part 313C, plate D, and the uncracked part 309 and the data were compared to the requirements of MIL-A-46100.

Centerline Rockwell C hardness (HRC) tests were performed on samples taken from part 313C, uncracked components which were subjected to stress relief heat treatments after cutting, and plate D. Hardness readings on the machined Charpy and tensile bars served to verify these centerline readings. To determine the effects of the various plate cutting procedures, Knoop microhardness tests were performed in 0.01-inch increments in from the cut edge on samples from plates cut by each of three processes: gas-shielded plasma, water-shielded plasma, and cold shearing. The Knoop hardness numbers were then converted to Rockwell C for ease of comparison.

Environmental Assisted Cracking Tests

In order to determine the environmental assisted cracking susceptibilities of Mn-Mo-B and Ni-Cr grades of high hardness steel, plane-strain stress corrosion tests were performed on material from part 313C and plate D. For each material, a series of six precracked cantilever-beam specimens (6" x 0.05" x 0.25") were subjected to various static cantilever loads. Each of these different loads correspond to different initial stress intensity and the time-to-failure of each specimen, when placed in a distilled water environment, was measured. A plot of initial stress intensity versus time-to-failure was made, and the K_{IEAC} was taken as the asymptote of the curves at 1,000-hour life.

The susceptibility of the Mn-Mo-B grade of material (part 313C) to environmental assisted crack initiation was also examined by testing a series of smooth, round bar specimens in atmospheres ranging from 0% to 100% relative humidity. Fractographic analysis was used to assess the crack initiation morphology.

RESULTS AND DISCUSSION

The susceptibility of high strength armor plate to stress corrosion cracking is well documented in the open literature¹⁻³ and MIL-A-46100 armor plate is no exception. The current failure analysis indicates environmental assisted cracking. Since the phenomenon can be best described by looking at the four characteristic conditions of crack initiation, environmental interaction, stress, and material susceptibility, the best way to present the experimental results is to investigate each condition separately. The four different areas will then be brought together in the summary.

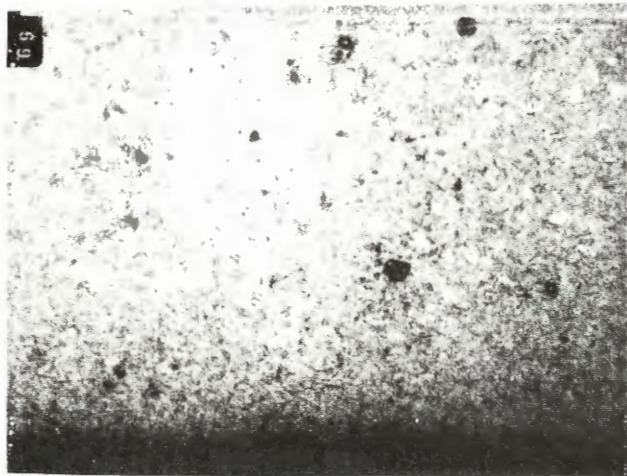
Crack Initiation

When 5/16-inch-thick high hardness steel was incorporated into production, oxyfuel cutting became an unacceptable method of cutting detailed parts because of the wide heat affected zone (HAZ). This HAZ is deleterious because the region is ballistically inferior to the harder base material. Therefore, alternate cutting procedures were implemented by the vehicle manufacturer to reduce the HAZ size while still maintaining satisfactory production rates.

These alternate methods, water-shielded plasma and cold shearing, were successful in reducing the HAZ size. However, they caused severe edge cracking on the as-cut detail parts (Figure 2). When water-shielded plasma was used, the rapid cooling of the cut edge produced a very narrow HAZ (30 mil), with a thin (5 to 10 mil) layer of untempered martensite at the cut edge. The formation of this martensite in conjunction with the high cooling rates resulted in the formation of quench cracks at 90° to the plate surface. Analogously, cold shearing of the plates introduced large amounts of mechanical deformation which over stressed the material and cracked the edge at a 45° angle (Figure 2).

Materials Characterization/Environmental Influence

The high hardness steel armor was procured to MIL-A-46100, and the chemistry and baseline mechanical properties of the plates involved with this study are given in Tables 3 and 5. The specimens taken from part 313C, which had a catastrophic crack, had a carbon level that was slightly above the specification range (0.28 to 0.32) and as a result the mechanical properties were also on the high side (HRC 55, UTS = 290, 0.2% YS = 220 ksi). However, despite the unusually high strength levels, the -40°F impact and room temperature fracture toughness values are satisfactory, and consistent with values typically seen for high hardness armor plate (14 ft-lb and 65 ksi $\sqrt{\text{in.}}$). The bulk structures of the 313C cracked part is martensitic (Figure 3), with spheroidized inclusions and little evidence of microstructural banding or any other inherent defect (such as stringers) which could account for the type of gross cracking observed in the as-cut parts. It should be noted, however, that the plates were tempered at 150°F for 15 minutes in warm water, and this fact set the stage for the EAC phenomenon because the majority of the quench-induced stresses remained in the plate after tempering.



140X

a. Mechanical Shearing

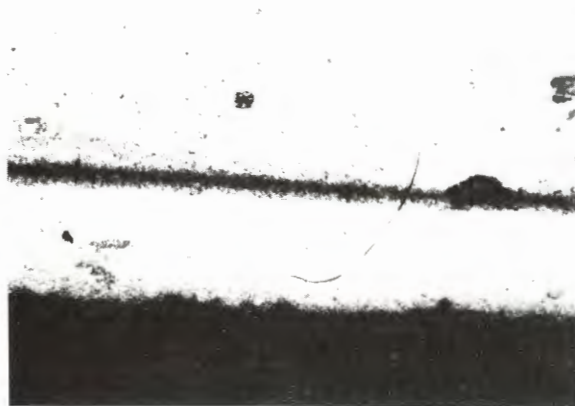
20 μ m



350X

b. Water-Shielded Plasma

10 μ m

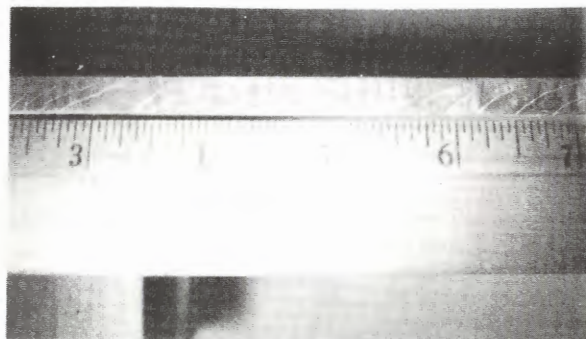


35X

c. Gas-Shielded Plasma

1 μ m

Two of three cutting processes used caused edge cracks up to 0.09 inch in length.
These microcracks function as EAC initiation sites.



d. Magnetic Particle Inspection of Plate Edge in a.

Figure 2. Comparison of Cut Edges



500X

Cracked Plate, Mn-Mo-B

20 μm



500X

Cracked Plate, Mn-Mo-B

20 μm



500X

Uncracked Plate, Mn-Mo-B

20 μm



500X

Raw Stock, Ni-Cr

20 μm

1. Tempered martensite microstructure seen in all samples.
2. Inclusions are spheroidized.
3. No inherent material deficiency (i.e., banding) can be linked to the cracking phenomenon.

Figure 3. Comparison of Microstructures.

Table 5. CHEMISTRY AND PROPERTY DATA ON HIGH-HARD STEEL

	0.2% YS (ksi)	UTS (ksi)	Elong. (%)	RA (%)	HRC	-40°F CVN (ft-lb)	K _{IC} (ksi√in.)	K _{IEAC} (ksi√in.)
313C Mn-Mo-B	220.0	289.0	8.9	36.0	55.0	15.0	68.5	15.0 (Distilled Water)
D Ni-Cr	222.0	276.0	7.5	42.3	50.0	15.0	64.5	13.0 (Distilled Water)
4340*	230.0	280.0	12.0	39.0	51.0	15.0	60.0	12.0 (Distilled Water) 8.0 (Sea Water)
J13 (Ref. 2)	207.0	255.0	13.3	51.8	51.0	-	99.0	15.7 (Distilled Water) 23.0 (3.5% NaCl)
G11 (Ref. 2)	208.0	262.0	13.5	49.8	50.0	-	83.0	15.8 (Distilled Water) 17.2 (3.5% NaCl)

*ASM Metals Handbook, v. 1, 9th Edition, 1978.

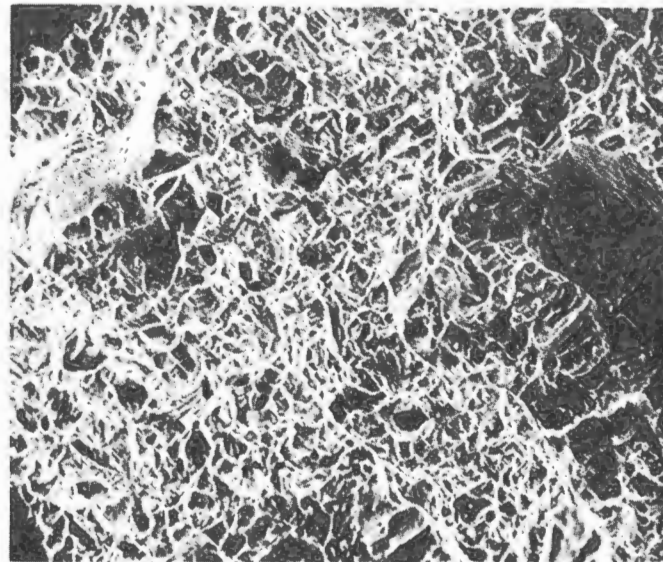
For comparison, a nickel-chromium grade of high hardness armor was examined and similar results, both microstructurally and mechanically, to the Mn-Mo-B grade were obtained (Table 5 and Figure 3). Since the Ni-Cr grade of high hard is a richer alloy (Table 3), it is typically tempered at higher temperatures. This reduces the relative tendency for EAC to occur. However, it is felt that if Ni-Cr and Mn-Mo-B high-hard steels are processed in exactly the same manner, both will possess similar susceptibilities to EAC.

Crack tips from cracks ranging in length from 0.25 inch to 7.0 inches from parts 313A, B, and C were examined by optical microscopy and SEM, and the fracture surfaces were compared to tensile and Charpy bar fracture surfaces. The tensile and Charpy bars failed through microvoid coalescence regardless of the test temperature (Figure 4), while the service cracks are clearly intergranular regardless of crack length (Figure 5). The implication of this result is that high hardness armor will not fracture in an intergranular manner, but rather through microvoid coalescence under normal, ambient conditions.

Since it seems that a different type of fracture mechanism is operative under service/fabrication conditions, a series of humid tension tests were run at room temperature to determine the susceptibility of the material to crack initiation. The resulting properties under various conditions of humidity were consistent with the results obtained under ambient conditions (Table 6). In addition, the classic "cup-cone" fracture morphology in the necked region was seen, as well as microvoid coalescence across the entire fracture surface. Therefore, it can be concluded that the material is not susceptible to EAC crack initiation.

Table 6. HUMID TENSILE TESTS

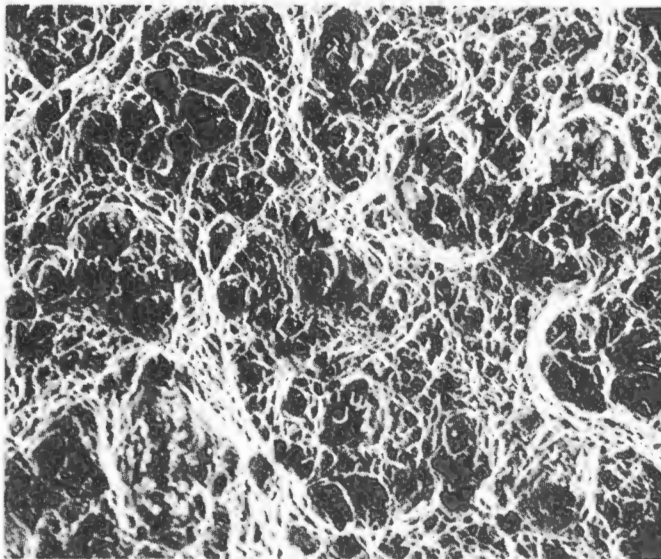
Base Material - Part 313C		
Humidity (%)	RA (%)	UTS (ksi)
0 (Ambient)	36.0	289.0
35	43.6	297.5
85	43.8	289.8
100	45.0	287.3



450X

Charpy Bar, 60°C, Mn-Mo-B

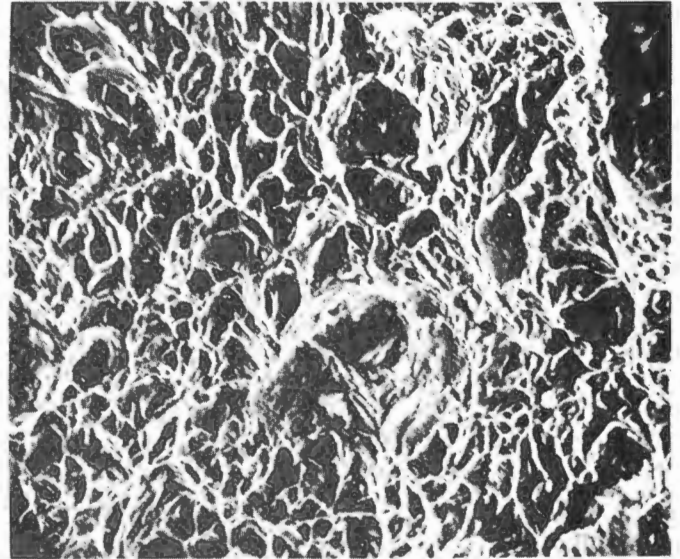
20 μ m



450X

Charpy Bar, 100°C, Mn-Mo-B

20 μ m



450X

Tensile Bar, RT, Mn-Mo-B

20 μ m

Figure 4. Comparison of Fracture Surfaces.

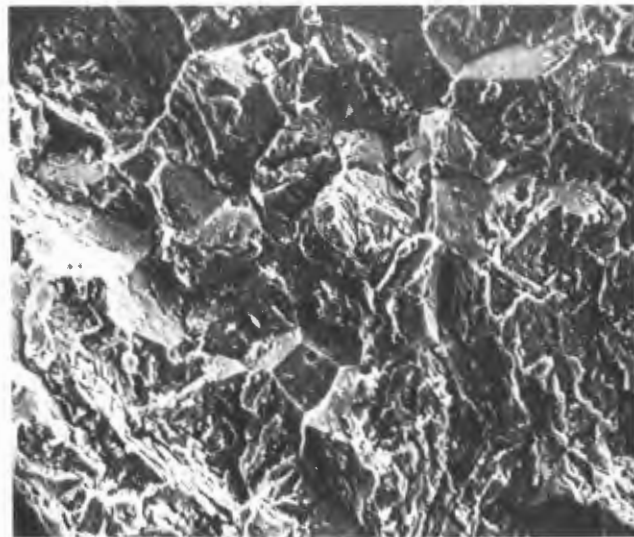
It appears therefore, that the susceptibility of high hardness armor to EAC is linked to a preexistent crack interacting with sufficient levels of stress to cause crack propagation in the ambient environment. Table 5 shows data for a series of different high strength materials tested under various environments and all the materials with similar strength levels show stress corrosion fracture toughnesses of 15 to 20 ksi $\sqrt{\text{in}}$. These data are consistent with Dawson and Levy,² who have suggested that the susceptibility of a material to EAC is not dependent on the type of environment, but rather on the material strength, with the susceptibility increasing with the yield strength.



425X

Optical Metallography of Crack Tip
from 0.030 inch Crack

20 μ m



850X

SEM of Crack Tip
from 2 inch Crack

10 μ m

Figure 5. Fracture surfaces of service crack.

In order to confirm this strength dependency of K_{IEAC} , cantilever beam K_{IEAC} tests were performed on material from both Ni-Cr and Mn-Mo-B grades of high hardness steel. The time-to-break was measured and the results are plotted in Figure 6. The asymptote of these stress intensity versus time-to-fracture curves at 1000-hour life were taken as the K_{IEAC} , and both grades of high hard displayed threshold stress intensities of 10 to 15 $\text{ksi}\sqrt{\text{in.}}$, which is consistent with the values given in Table 5.

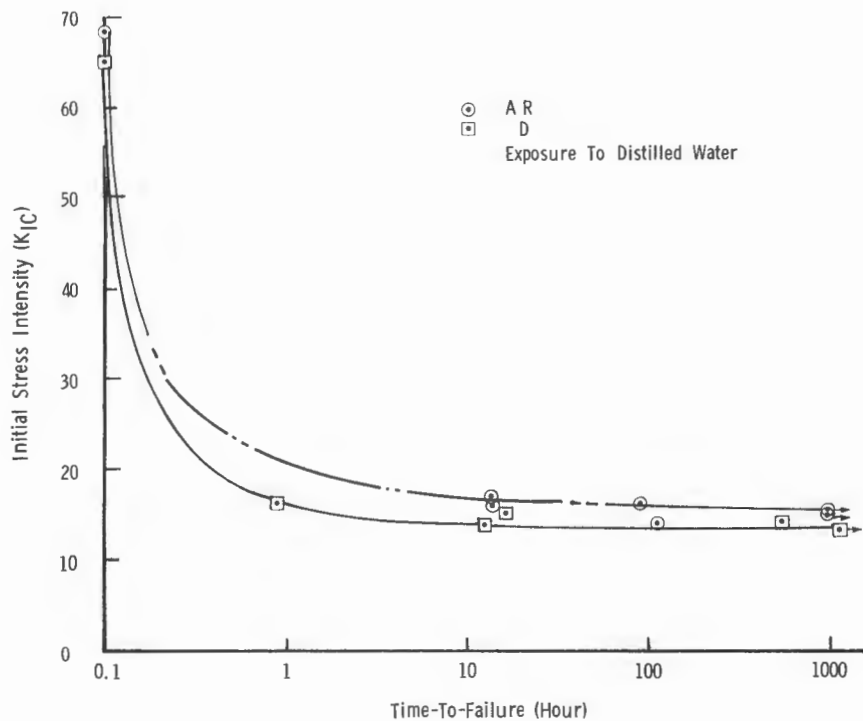


Figure 6. K_{IC} - time-to-break curves.

The low K_{IEAC} values indicate clearly that the armor that failed during fabrication, as well as the Ni-Cr grade, are both highly susceptible to EAC when a pre-existing crack is exposed to an aggressive environment and this material is not susceptible to EAC crack initiation. Therefore, one alternative is to cut the parts in a way that avoids introducing edge cracks. Gas-shielded plasma is a thermal cutting process that can provide a narrow HAZ along with slower cooling rates than water-shielded plasma. In this way, the good points of both water-shielded plasma (speed of cut) and oxyfuel (slower cooling) cutting are achieved without initiating cracking at the cut edge. This approach was tried in production, and edge cracks were avoided, but the gas-shielded plasma technique became an undesirable option due to excessive smoke and high-noise levels.

Changing the cutting method is only a short-run solution, because if a crack is introduced at some later point, (e.g., due to a ballistic impact), it will propagate by EAC. Therefore, the best way to approach the problem is to minimize the stress level in the plate in order to reduce the tendency for crack propagation.

Residual Stress

In order for edge cracks (caused by detail part cutting) to propagate under the influence of the environment (ambient humidity), there must be a tensile stress (either applied or residual). Since no significant external loads were placed on the high hardness steel plates studied, residual tensile stresses are indicated. Two sources of residual stress in high hardness steel parts are the heat treatment process used to produce the plate, and the thermal cutting process used during the fabrication of the plates.

It is generally accepted that the quenching during heat treatment is a primary source of residual stress, while tempering relieves the quenched stresses. During quenching of armor steel, the plate is restrained to prevent dimensional distortion (variations in flatness and excessive waviness of the plate) either by a platten quench press or by a roller quench press. This macroscopic restraint coupled with the microscopic lattice distortion of the martensitic transformation will create residual stress in the plate.

X-ray diffraction measurements⁶ showed that compressive stresses were present⁷ due to shot blasting of the part.⁸ However, tensile stress had to be present for the crack to propagate.

Tempering

Tempering of quenched plates not only allows carbide formation in martensite, it also allows stress relaxation to occur. This investigation examined macrostress relaxation in tension specimens at typical high hardness steel tempering temperature (150°F to 400°F) with the test set-up shown in Figure 7. Two initial applied stresses (200 ksi and 100 ksi) were examined, and the stress-time dependence can be seen in Figure 8. Both curves have several common factors. First, the higher the temperature the greater the stress relieved. Second, the majority of the stress relief occurs within the first 30 minutes of tempering, with practical maximum

6. CULLITY, D. B. *Elements of X-Ray Diffraction*. 2nd ed., Addison-Wesley Pub., Reading, MA, 1978, Chapter 16, p. 447-476.

7. GAZZARA, C. *X-Ray Residual Stress Analysis of Steel Armor Plate No. 312 Part II*. Letter Report, 22 March 1983.

8. WOHLFAHRT, H. *Shot Peening and Residual Stresses* in Residual Stress and Stress Relaxation, Proceedings of 28th Sagamore Army Materials Conference, 1982, p. 71-92.

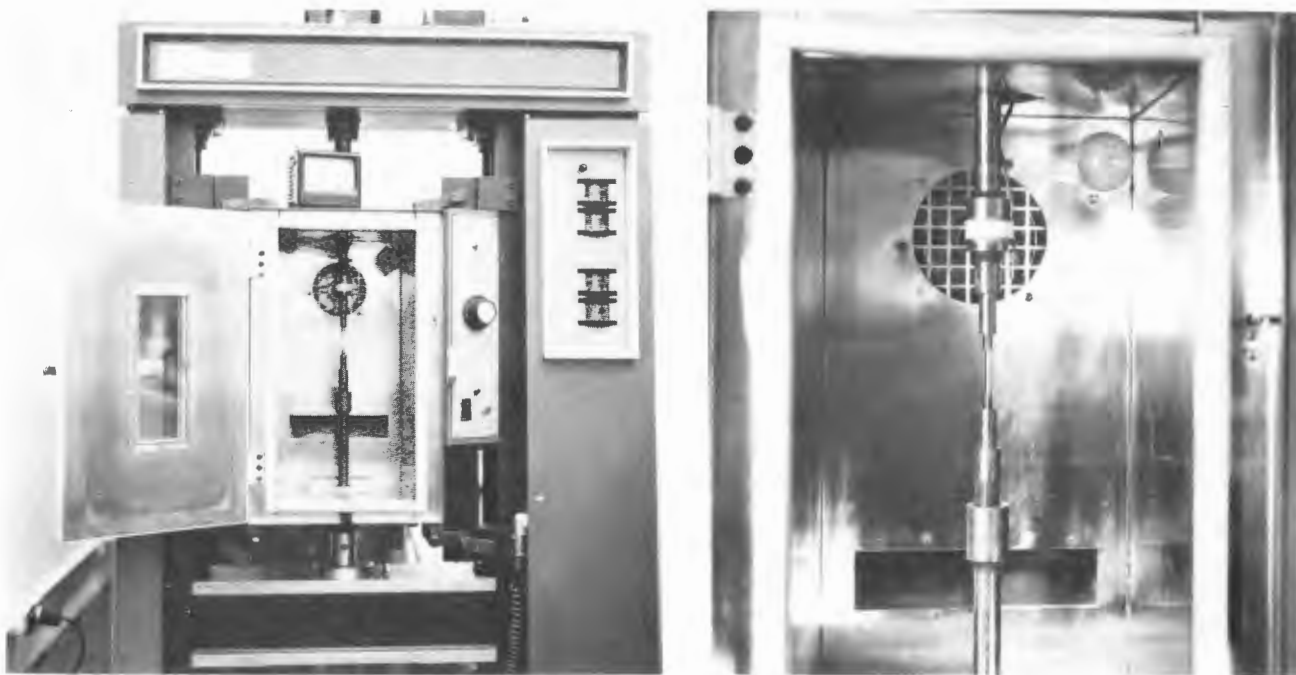


Figure 7. Stress relaxation test fixture.

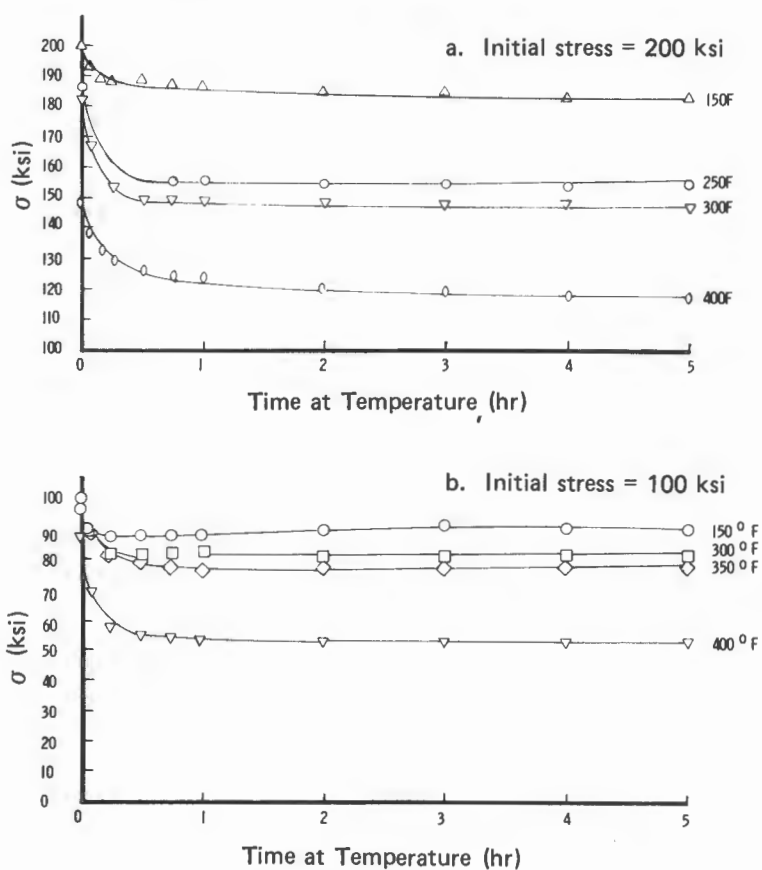


Figure 8. Stress relaxation results.

stress relief occurring after one hour. Theories of stress relief relate the mechanism to either the tempering process (microstructural changes) or dislocation motion (a low temperature creep phenomena). Brown and Cohen,⁹ in their studies used a split ring type of specimen to relate percent stress relieved to tempering temperatures and times in an AISI 52100 steel. They found that maximum stress relief occurred after one hour and the magnitude increased with tempering temperature. Their use of a significantly higher carbon steel however, precludes a direct comparison. Another explanation for stress relief is by a low temperature creep type of dislocation motion. Discussions of low temperature creep¹⁰ relate strain (in this case stress relaxation at fixed strain) to dislocation activity. Dislocation motion is thermally activated, and no regeneration occurs. Hence, for a specific temperature there is a fixed amount of stress relief, and increasing temperature would increase the number of active dislocations and therefore the magnitude of the stress relieved. In summary, both explanations of stress relief mechanisms are consistent with the finding of this study that increasing tempering temperature will increase stress relaxation and maximum stress relief occurs after a finite time.

High hardness steel specification (MIL-A-46100) requires a hardness of HRC 48 to 52, and a maximum carbon content of 0.32%. These combined requirements make it necessary to allow as low a tempering temperature as possible. A minimum tempering condition of 30 minutes at 350°F was chosen in order to maximize stress relaxation without compromising hardness, or requiring uneconomical times in the furnace. This minimum tempering requirement was presented at the June 1983 specifications meeting, and was accepted by government and industry representatives. It was incorporated into revision C of MIL-A-46100. It should be noted the 30 minutes at 350°F is the time at temperature at the plate centerline, so plates substantially thicker than the 5/16-inch plate studied here would require furnace times longer than 30 minutes, e.g., a 2-inch plate would require three hours in the furnace to have the centerline be at 350°F for 30 minutes.

SUMMARY

The cracking of the 5/16-inch armor plate (MIL-A-46100) has been shown to be a representative example of environmental assisted cracking, where an edge crack introduced by a fabrication process interacted with the moisture in the ambient environment and bulk plate residual stress to promote stable, subcritical crack propagation.

Since the four necessary conditions are interdependent and must exist simultaneously, several approaches to avoiding the EAC problem have been addressed in this study. First, and most simple, if the cutting procedure is controlled to avoid edge cracking, there will be no EAC because preexistent cracks are absent. This however, is a shortsighted approach, because if at some later point during the life of the vehicle a crack is introduced, EAC will become operative.

9. BROWN, R. L., RACK, H. J., and COHEN, M. *Stress Relaxation During the Tempering of Hardened Steel*, Materials Science and Engineering, v. 21, 1975, p. 25-34.

10. DIETER, G. E. *Mechanical Metallurgist*, McGraw-Hill Co., New York, 1976, Chapter 13, p. 451-487.

Second, and still relatively shortsighted, is to subject all as-cut parts to a post cut stress relief heat treatment (PCSRHT) in order to lower the bulk stresses in the detailed parts, as well as any stress gradient at the part edge due to thermal cutting. However, if a crack is present in the detail part, there is no guarantee that the PCSRHT has been completely successful, and the crack may still propagate, although at a reduced rate. Furthermore, the PCSRHT will invariably lower the bulk hardness of the detail part by 1 to 2 HRC, and careful track must be kept of the initial hardness to ensure that the parts are not oversoftened below the minimum required in MIL-A-46100.

The most farsighted approach to controlling EAC is to limit the level of quench-induced residual stress in the bulk plates during heat treatment in the steel mill. The high hardness armor of this study was, in retrospect, defective in the sense that the tempering parameters of 150°F/15 min were virtually ineffectual with respect to any significant reduction of stress (Figure 8). However, if these same plates had been tempered with the recommended temperature-time parameters, adequate reductions of plate stress would have been achieved. Through this methodology, even if a small fabrication-induced edge crack exists, it will not grow because there is no driving force (e.g., residual stress levels are too low). Analogously, by lowering the plate stresses, the instantaneous stress intensity of the crack tip is below the stress corrosion fracture toughness.

Revision C of MIL-A-46100 incorporates a change which requires a minimum treatment of 350°F for 30 minutes as a final heat treatment operation.

This modification to the specification has been successful in that no reports of catastrophic cracking of high-hard plates during vehicle construction have been made since June 1983, when revision C of MIL-A-46100 became effective.

More research is required, however, to ensure that the specified minimum temperature and time are sufficient. The stress relaxation experiments conducted in this study indicate that these tempering conditions should result in a reduction of bulk plate stress levels of approximately 25%. Further studies are needed to measure typical residual stress levels in as-quenched and in tempered plate produced by the various industrial roller and platten quench facilities. Fracture mechanics could then be used to specify combination of tempering conditions and maximum length of edge cracks introduced by plate cutting to maintain $K_{IC} < K_{IEAC}$.

DISTRIBUTION LIST

No. of Copies	To
1	Office of the Under Secretary of Defense for Research and Engineering, The Pentagon, Washington, DC 20301
	Commander, Army Research Office, P.O. Box 12211, Research Triangle Park, NC 27709
1	ATTN: Information Processing Office
	Commander, U.S. Army Materiel Command, 5001 Eisenhower Avenue, Alexandria, VA 22333
1	ATTN: AMCLD
	Commander, U.S. Army Tank-Automotive Command, Warren, MI 48090
1	ATTN: AMCPM-GCM-SA, Mr. Ralph Polson
2	AMSTA-UL, Technical Library
1	AMCPM-GCM-SA, Mr. Joe Roosen
	Commander, U.S. Army Foreign Science and Technology Center, 220 7th Street, N.E., Charlottesville, VA 22901
1	ATTN: Military Tech, Mr. Marley
	Director, U.S. Army Ballistic Research Laboratory, Aberdeen Proving Ground, MD 21005
1	ATTN: Dr. W. Gillich
1	G. Filbey
1	N. Ruppert
	General Dynamics Corporation, Land Systems Division, P.O. Box 1804, Dept. 8292, Warren, MI 48090
1	ATTN: Mr. William Potrafke, MZ 498-03-06
	General Dynamics Corporation, Land Systems Division, P.O. Box 1901, Warren, MI 48090
1	ATTN: Richard Auyer
	FMC Corporation, Central Engineering Lab, Coleman Avenue, Santa Clara, CA 95050
1	ATTN: Mr. Paul Das
1	Mr. Gary Boerman
	Lukens Steel Company, Coatesville, PA 19320
1	ATTN: Dr. W. Nachtrab
	United States Steel Corporation, Physical Metallurgy Labs, Homestead, PA 15120
1	ATTN: Mr. Jerry Jim
	Director, Army Materials and Mechanics Research Center, Watertown, MA 02172-C001
2	ATTN: AMXMR-PL
5	Author